The influence of carbon and nitrogen on the electronic structure and hyperfine interactions in face-centred-cubic iron-based alloys

2001 J. Phys.: Condens. Matter 13 1051

(http://iopscience.iop.org/0953-8984/13/5/318)

INSTITUTE OF PHYSICS PUBLISHING JOURNAL OF PHYSICS: CONDENSED MATTER

J. Phys.: Condens. Matter **13** (2001) 1051–1061 www.iop.org/Journals/cm PII: S0953-8984(01)16178-3

The influence of carbon and nitrogen on the electronic structure and hyperfine interactions in face-centred-cubic iron-based alloys

A N Timoshevskii[1,3], **V A Timoshevskii**[2] **and B Z Yanchitsky**[1]

[1] Institute of Magnetism, 36-b Vernadskii Street, 252680 Kiev, Ukraine
[2] Rostov State University of Transport, Narodnogo Opolcheniya 2, Rostov-on-Don, 344038, Russia

Received 8 August 2000, in final form 29 November 2000

Abstract

Carbon and nitrogen austenites, modelled by Fe_8N and Fe_8C superstructures, are studied by the full-potential linearized augmented-plane-wave (LAPW) method. Structure parameters, electronic and magnetic properties, as well as hyperfine interaction parameters are obtained. Calculations prove that Fe–C austenite can be successfully modelled by the ordered Fe_8C superstructure. The results show that the chemical Fe–C bond in Fe_8C is more covalent than the Fe–N bond in Fe_8N. A detailed analysis of electric field gradient formation is performed for both systems. The calculation of the electric field gradient permits an interpretation of the Mössbauer spectra for Fe–C and Fe–N systems.

1. Introduction

Face-centred-cubic (fcc) iron-based alloys are widely used for developing stainless austenitic steels especially for use in critical temperature ranges, aggressive environments and other severe external conditions. Doping of these steels with light interstitial impurities influences the mechanics and kinetics of structural phase transitions in Fe-based alloys. Nitrogen doping helps to solve the problem of how to strengthen stainless steels.

Carbon and nitrogen doping influence the structure and mechanical properties of austenites differently. Study of this effect by means of Mössbauer spectroscopy determined substantial differences between the spectra of carbon and nitrogen austenitic steels (Sozinov *et al* 1997, 1999). The wealth of information contained in the Mössbauer spectra, as well as the high accuracy of the measurements, makes a detailed interpretation of these experimental results a complicated problem which requires the application of accurate theoretical methods.

The role of *ab initio* calculations in the area of solid-state research has expanded rapidly during the last few years. Step by step, semiempirical methods containing many parameters are being replaced by calculations from first principles. We currently observe an extensive application of *ab initio* quantum mechanical methods in calculations of the electronic structure

[3] Author to whom any correspondence should be addressed.

0953-8984/01/051051+11$30.00

and physical properties of solids. These methods are increasingly used for solving not only fundamental, but also applied problems.

In this paper we study the influence of carbon and nitrogen on the atomic and electronic structure of fcc iron. Mössbauer spectroscopy gives the most interesting data on the impurity distributions, electronic structure and magnetic interactions in solids. The study of shifts and splittings of nuclear energy levels gives information about the symmetry of the charge distributions near the nucleus, the electronic configurations of atoms and ions and peculiarities of the atomic structure of solids. We believe that a detailed interpretation of these experimental data using an up-to-date *ab initio* approach is an important step in the investigation of the influence of light impurities (C, N) in the case of fcc iron-based alloys.

2. Atomic structure

Up to now there has been no full understanding of the influence of carbon and nitrogen atoms on the atomic and electronic structure of fcc Fe–C and Fe–N alloys. On the basis of Mössbauer spectroscopy data, different authors drew different conclusions about the atomic structure of Fe-based carbon and nitrogen fcc alloys. For example, the group of Genin concluded that the carbon distribution in fcc Fe–C alloys is close to the ordered Fe_8C_{1-x} structure (Bauer *et al* 1990). On the other hand, the group of Gavriljuk, using another method of deconvolution of the Mössbauer spectrum and performing Monte Carlo computer simulations, showed that formation of the ordered Fe_8C_{1-x} structure is improbable (Sozinov *et al* 1997).

In this paper we study these alloys theoretically, choosing the ordered Fe_8C and Fe_8N superstructures as models for our investigations. This approach permits a determination of the differences between the influence of carbon and nitrogen on the electronic structure of fcc iron. In the present research we are trying to solve two problems: to study the differences in electronic structure of carbon and nitrogen austenites; and to perform a detailed interpretation of experimental Mössbauer data for Fe–N and Fe–C alloys.

Calculations were performed with the WIEN97 program package (Blaha *et al* 1999), which employs the full-potential LAPW method (Singh 1994a). The generalized gradient approximation (GGA) according to the Perdew–Burke–Ernzerhof (Perdew *et al* 1996) model was used for the exchange–correlation potential. The value of the plane-wave cut-off was $R_{mt}K_{max} = 8.4$, which corresponds to about 190 plane waves per atom in the basis set. Inside the atomic spheres the wave function was decomposed up to $l_{max} = 12$. The charge density and potential were decomposed inside the atomic spheres using a lattice harmonics basis up to $L_{max} = 6$. In the interstitial region a Fourier expansion with 847 coefficients was used. Calculations were performed for 3000 k-points in the Brillouin zone. The radii of the atomic spheres were chosen as 1.9 au for Fe atoms and 1.6 au for N and C atoms. The standard LAPW basis set was expanded by including local orbitals (Singh 1994b) for the Fe 3s3p states and the N and C 2s states. The values of all parameters were tested for convergence and an accuracy of 0.1 mRyd of the total energy of the system was achieved. In order to take into account the role of local magnetic moments for the Fe atoms, all calculations were performed using the spin-polarized approximation.

Figure 1 shows the Fe_8A supercell ($Fm\bar{3}m$, No 225), which was used for the calculations. The structure has Fe atoms of two symmetry types: Fe_1-type atoms form an octahedron around an impurity atom—i.e. they have one impurity atom in the first coordination sphere; Fe_0-type iron has no impurity atoms in the first coordination sphere. Before we performed the final calculation of the electronic structure and hyperfine interaction parameters, a total-energy-minimization procedure was performed to obtain the equilibrium positions of the atoms. The lattice constant as well as the size of the Fe_1 octahedron were varied to obtain the total-energy

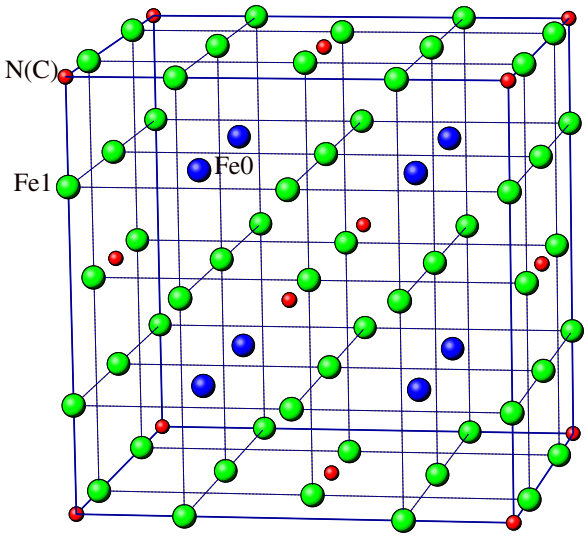

Figure 1. Ordered Fe_8A superstructures (A = C, N). Atoms Fe_1 have one impurity atom in the first coordination sphere. Atoms Fe_0 have no impurity in the nearest neighbourhood.
(This figure is in colour only in the electronic version, see `www.iop.org`)

minimum. The optimization results were approximated by second-order polynomials using a least-squares fitting method. Then we found the values of the lattice parameters and positions of the atoms of the Fe octahedron analytically. Calculated and experimental values of the lattice parameters as well as the calculated distances between Fe and C (N) atoms are presented in table 1. Optimization results for iron nitride, Fe_4N, are also presented. The good agreement with experiment shows that the method can be successfully applied to iron–nitrogen (iron–carbon) compounds.

Table 1. Structure parameters and magnetic moments for Fe_8N, Fe_8C and Fe_4N compounds. Fe–A is the distance between the Fe and the impurity atom (au) and μ is the local magnetic moment (μ_B).

	Lattice parameter	Fe–A distance	μ_{Fe_0}	μ_{Fe_1}	μ_{Fe_2}	$\mu_{N,C}$	μ (average/ atom)
Fe_8N (theory)	13.946	3.54	2.78	2.09	—	−0.11	2.25
(experiment)	13.849[a]						
Fe_8C (theory)	13.981	3.58	2.71	2.12	—	−0.16	2.25
(experiment)	13.839[a]						
Fe_4N (theory)	7.164	3.582	2.90	—	2.31	0.04	2.50
(experiment)	7.171[b]	3.585[b]	3.00[c]	—	2.00[c]		2.21[c]

[a] Cheng *et al* (1990).
[b] Jacobs *et al* (1995).
[c] Frazer (1958).

3. Electronic structure

Figure 2 presents the total and partial densities of states for Fe, C and N atoms in Fe_8A compounds. The main difference between the electronic structures of the two compounds is as regards the energy of the impurity 2p states. In Fe_8C, carbon 2p states are located right

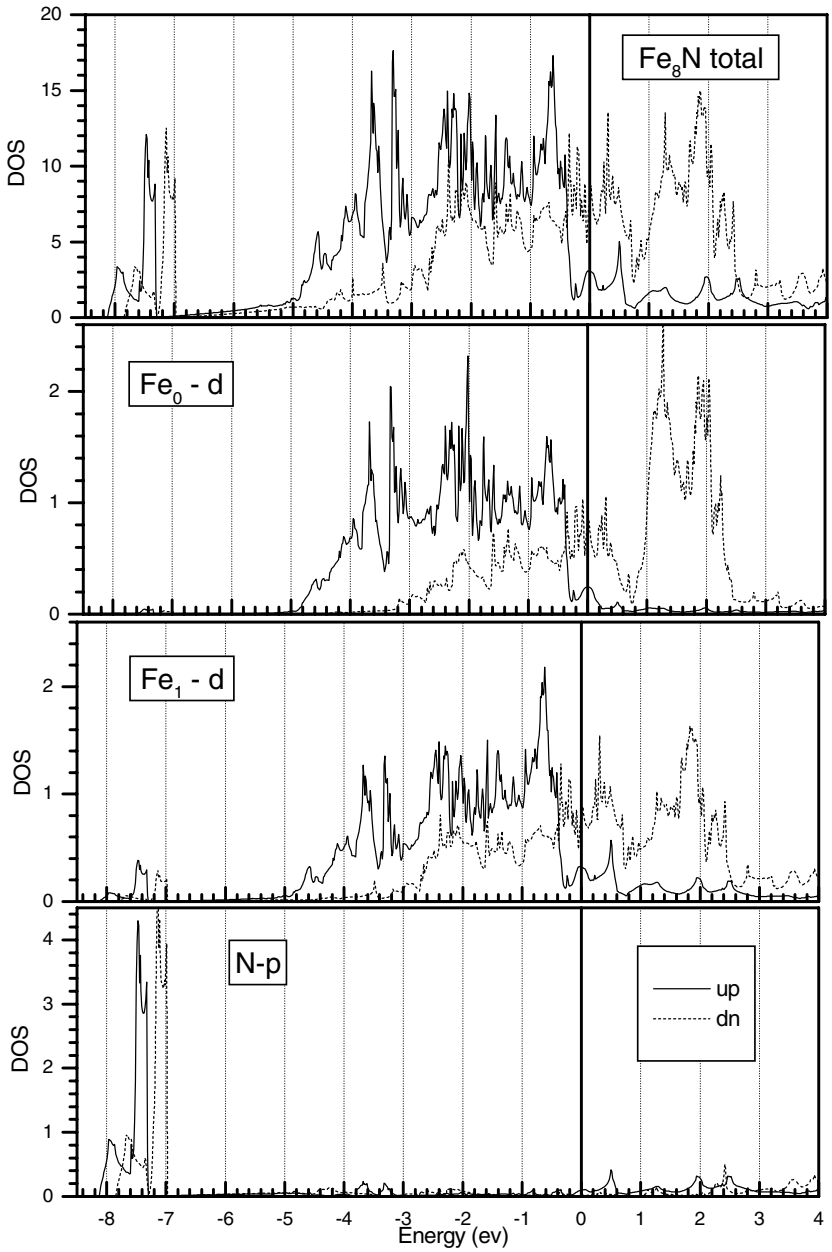

Figure 2. Densities of states (DOS) for Fe_8A (A = C, N) compounds.

below the d band of iron. In Fe_8N, nitrogen 2p states are located 2 eV below the bottom of the Fe d band. This difference in energy of the C and N 2p states leads to an essential difference in character of the chemical bonding for these two compounds. In Fe_8C we see stronger p–d hybridization compared to the Fe_8N compound. The width of N 2p band is half that of the corresponding 2p band of carbon. This probably leads to a Fe–C interaction that is much stronger than the Fe–N interaction.

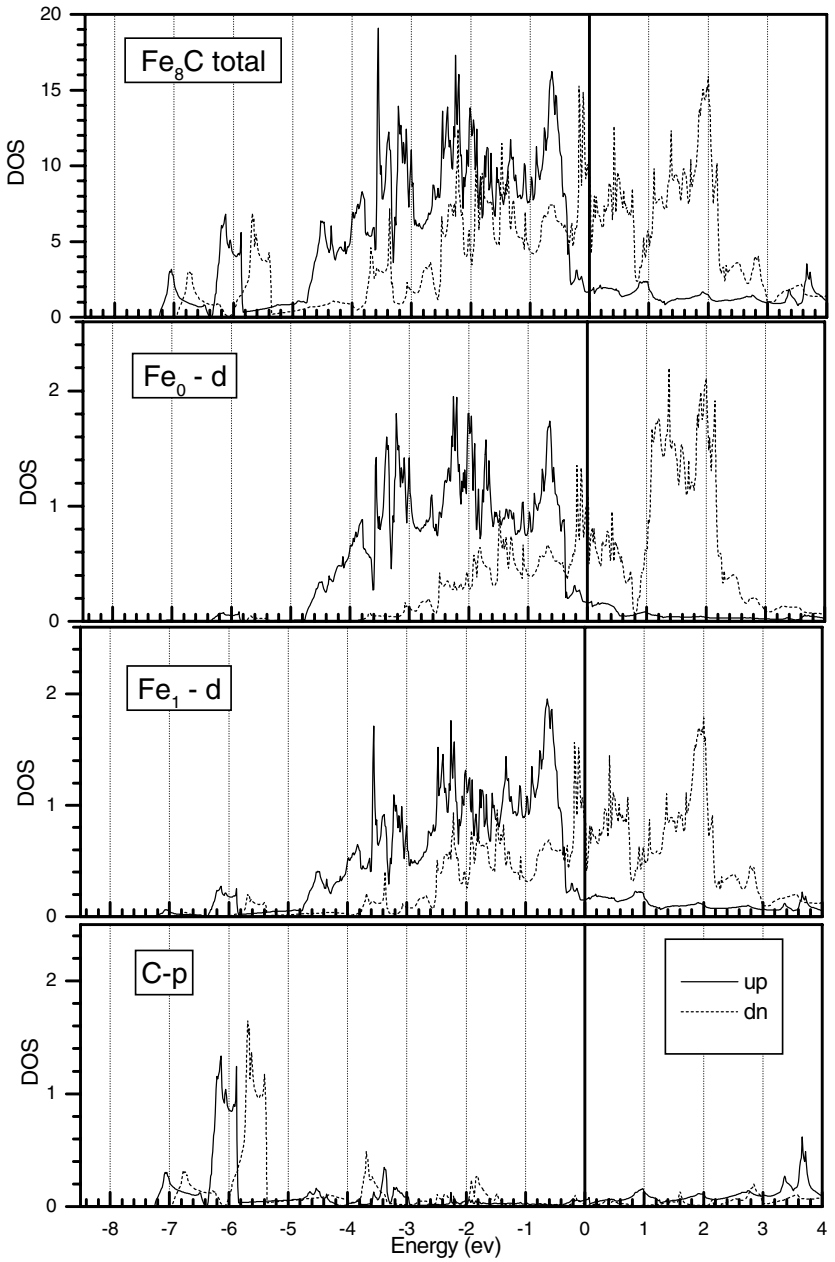

Figure 2. (Continued)

We also calculated the values of the local magnetic moments of Fe atoms for Fe_4N, Fe_8N and Fe_8C compounds. We observe a good agreement of the theoretical and experimental results for the iron nitride structure (table 1). To perform a detailed analysis of the role of the hybridization effect we calculated the contributions of different d orbitals to the formation of the local magnetic moments of the Fe atoms for Fe_4N, Fe_8N and Fe_8C structures. The results are presented in table 2. We see that the contribution of the d_{z^2} orbital is three times smaller for

Table 2. Contributions of different 3d orbitals to the formation of the local magnetic moments (μ_B).

	Atom	d_{z^2}	$d_{x^2-y^2}$	d_{xy}	d_{xz}	d_{yz}
Fe_4N	Fe_0	0.65	0.65	0.52	0.52	0.52
	Fe_2	0.20	0.53	0.47	0.50	0.50
Fe_8N	Fe_0	0.66	0.66	0.49	0.49	0.49
	Fe_1	0.32	0.53	0.44	0.40	0.40
Fe_8C	Fe_0	0.66	0.66	0.47	0.47	0.47
	Fe_1	0.33	0.55	0.45	0.41	0.41

the Fe_2 atom compared to the Fe_0 atom for the Fe_4N structure. In Fe_8N and Fe_8C structures we have Fe_1 atomic configurations, and for these types of atom the contribution of the d_{z^2} orbital is two times smaller compared to that for the Fe_0 atom. This effect is connected with strong hybridization of the d_{z^2} orbitals with the p_z states of nitrogen. This hybridization effect is substantially stronger in the case of the dumb-bell configuration, which is present in the iron nitride structure. It should be pointed out that we do not observe any substantial difference between the influences of the C and N impurity atoms on the formation of the local magnetic moments of the Fe atoms in Fe_8N and Fe_8C structures.

Our calculations show that the difference between the magnetic moments of the Fe_0 and Fe_2 atoms in the Fe_4N structure is 0.6 μ_B, while the experimental value of this difference is 1.0 μ_B (table 1). This can be explained by the fact that a large density of spin-down states of the Fe_2 atom is located in the interstitial region. This leads to the overestimation of the Fe_2 magnetic moment, which is calculated only inside the atomic sphere.

We should note that experimental investigation of the local magnetic moments in fcc iron-based alloys is a complicated problem. Several research groups tried to experimentally estimate magnetic properties of the fcc phase of iron (Prescia *et al* 1987, Montano *et al* 1987, Macedo and Keune 1988). Different researchers reported contradictory results. The situation is even more complicated for the binary Fe–N and Fe–C alloys. Up to now there has been no experimental information on local magnetic moments in these alloys. In this paper we are trying to make a kind of prediction in this field, which could be useful for future experiments.

The difference in energy distribution of the valence electrons leads to a considerable difference between the electronic density distributions in Fe_8N and Fe_8C. Figure 3 presents the electronic density distribution in the (100) plane for two energy intervals: the 2p states of impurity atoms and the 3d states of iron in Fe_8N and Fe_8C compounds. The nitrogen 2p electrons are much more localized (figure 3(a)) compared to the 2p electrons of carbon (figure 3(c)). The charge distribution around the Fe_1 atoms in Fe_8C is more symmetric (figure 3(d)) compared to the corresponding charge distribution in Fe_8N (figure 3(b)). It should be noted that impurity atoms cause an asymmetric charge distribution around the Fe_1 atom. This also leads to asymmetric distribution of the d electrons of Fe_1. These effects greatly influence the electric field gradient (EFG) at Fe_1 nuclei, which can be measured as a quadrupole splitting in Mössbauer spectra.

4. Hyperfine interactions in Fe_8N and Fe_8C

For our structures the quadrupole splitting of the ^{57}Fe nucleus is given by the expression

$$\Delta = \frac{1}{2} e Q V_{zz} \tag{1}$$

where Q is the quadrupole moment of the nucleus and V_{zz} is the principal component of the electric field gradient (EFG) tensor.

In our calculations we used $Q(^{57}\mathrm{Fe}) = 0.16$ b, as determined by Dufek *et al* (1995) by comparing experimental quadrupole splittings and calculated EFG values for a large number of different Fe compounds. The EFG is calculated on an *ab initio* basis directly from the electronic density distribution using the method developed by Blaha *et al* (1985).

Table 3 presents our results for the quadrupole splittings as well as experimental data for carbon and nitrogen austenites, obtained by several groups. We see that reasonable agreement with experiment is obtained for Fe–C alloy. This leads to the conclusion that the local environment of the Fe_1 atom in the real alloys is close to the Fe_1 environment in our model Fe_8C superstructure. This is also supported by the fact that according to experimental data (Bauer *et al* 1988, Gavriljuk and Nadutov 1983, Oda *et al* 1994), Fe–C austenite has only Fe_0 and Fe_1 atoms, which corresponds to Fe configurations in our model superstructure. On the other hand, for the Fe–N austenite the Mössbauer spectrum is formed by contributions from Fe_0, Fe_1 and Fe_{2-180° (dumb-bell configuration) atoms (Oda *et al* 1990, Foct *et al* 1988, Gavriljuk *et al* 1990). Both the absence of Fe_{2-180° atoms in our structure and the bad agreement with experiment show that Fe–N austenite probably cannot be modelled by the Fe_8N superstructure.

Table 3. Calculated and experimental values of the quadrupole splitting Δ (mm s^{-1}) in Mössbauer spectra for Fe–N, Fe–C fcc alloys.

	Fe_4N	Fe_8N	$Fe_{10.1}N$	$Fe_{11}N$	Fe_8C	$Fe_{11.3}C$	$Fe_{11.5}C$
Δ (theory)	0.50	0.18			0.53		
(experiment)	0.50[a]		0.39[b]	0.25[c]		0.64[d]	0.67[e]
				0.39[f]		0.63[g]	

[a] Rochegude and Foct (1986).
[b] Oda *et al* (1990).
[c] Foct *et al* (1988).
[d] Genin and Flinn (1968).
[e] Oda *et al* (1994).
[f] Gavriljuk *et al* (1990).
[g] De Cristofaro and Kaplow (1977).

Our calculation shows that the contribution to V_{zz}, the principal component of the EFG tensor, from the regions outside the spheres (lattice EFG) is 5%, 3% and 10% for Fe_8N, Fe_8C and Fe_4N respectively. So, to understand the origin of the EFG we focus on its main component, the valence EFG, which originates from the space inside the atomic spheres. The ingredients for the calculation of the valence EFG are the density coefficients ρ_{2M} (Blaha and Schwarz 1983), which originate from two radial wave functions with angular momenta l and l':

$$\rho_{LM}(r) = \sum_{E<E_F} \sum_{l,m} \sum_{l',m'} R_{lm}(r) R_{l'm'}(r) G_{Ll l'}^{Mmm'} \tag{2}$$

where $R_{lm}(r)$ are the LAPW radial wave functions and $G_{Ll l'}^{Mmm'}$ are the Gaunt integrals.

We performed a comparative analysis of EFG formation for Fe_8N and Fe_8C structures. Table 3 and table 4 show that the total EFG and quadrupole splitting are almost three times larger in the Fe_8C structure compared to Fe_8N. By performing an analysis of the mechanisms of EFG formation, we tried to find the reasons for this considerable difference. First of all, it is obvious that the contribution from the Fe 3s3p energy interval remains constant when going from the nitrogen to the carbon compound. This means that the redistribution of the electronic density in this region is not substantial and cannot influence the increase of the total EFG. We observe an increase of the negative contribution from the C 2s interval, but it is

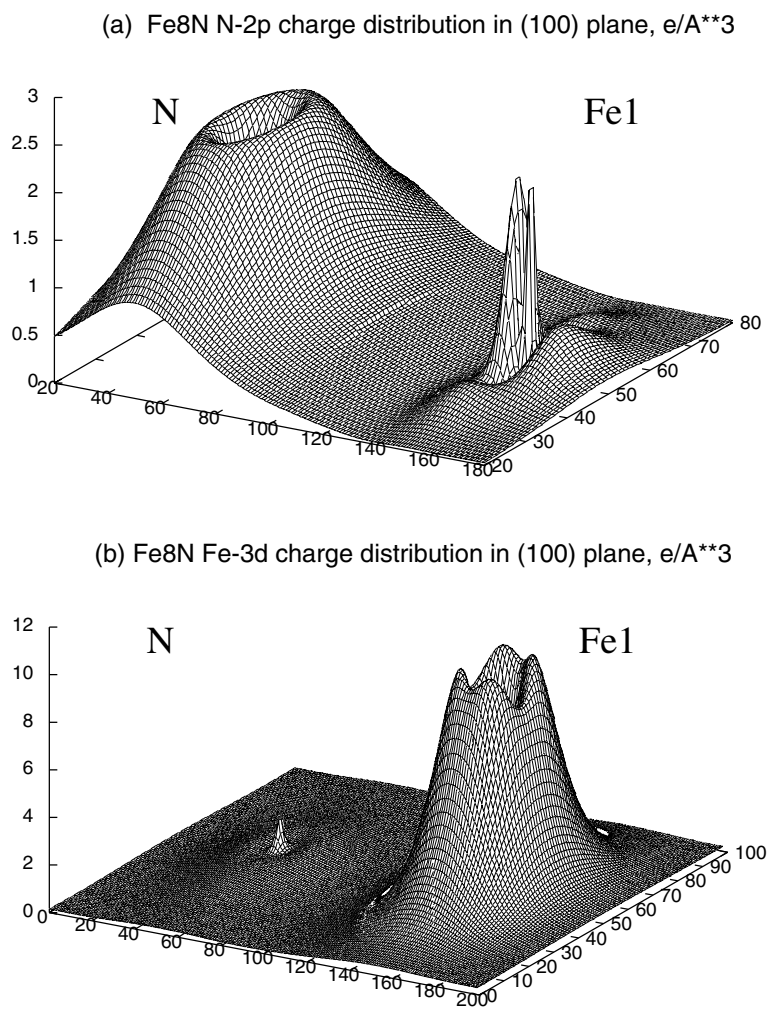

Figure 3. Fe_8N and Fe_8C charge distribution in the (100) plane ($e/\text{Å}^{-3}$) for different energy regions.

also not substantial. Moreover, the sum of the contributions from the impurity 2s2p energy interval remains almost constant when going from nitrogen to carbon. This means that the main reason for the increase of the EFG is the redistribution of charge density in the Fe 3d band (and partially in the impurity 2p band).

In Fe_8N, the 2p3d band EFG contribution is positive, which decreases the total EFG. In Fe_8C this contribution is negative and increases the total EFG. In Fe_8C, the charge distributions in the 2p and 3d bands are more symmetric than in Fe_8N. While going from N to C, the relative increase of the symmetry of the 3d charge distribution is much larger than the relative increase of the symmetry of the 2p charge distribution, which leads to a smaller EFG compensation and, as a result, to a negative contribution from the 2p3d band.

Let us now consider the partial contributions (p–p, d–d) inside the Fe_1 sphere. Other symmetry contributions—the s–d one etc—are negligibly small. While going from N to C, we observe a relatively small increase of the absolute value of the p–p contribution and quite

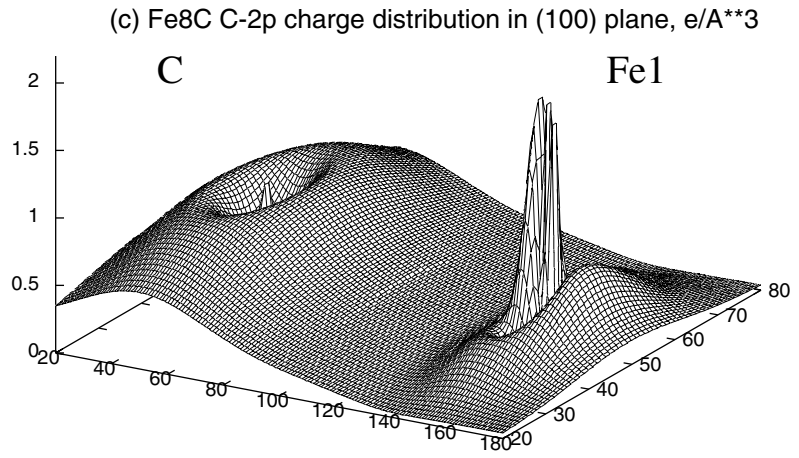

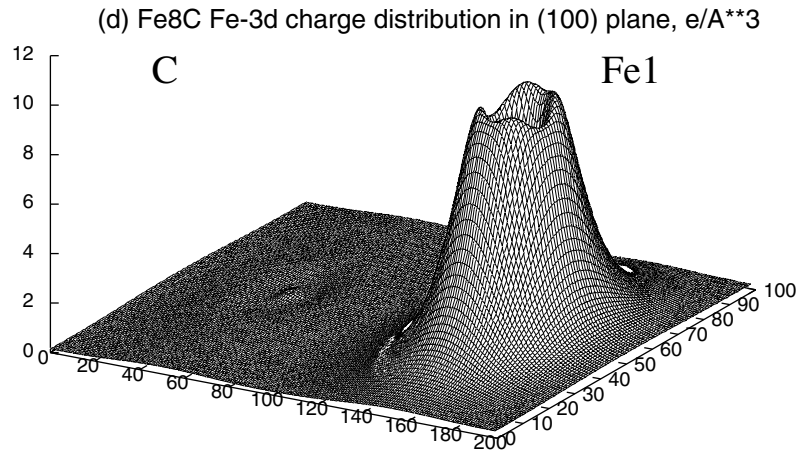

Figure 3. (Continued)

Table 4. EFG analysis for the Fe_1 atom in the Fe_8N and Fe_8C superstructures. Contributions to the valence EFG (10^{21} V m^{-2}) from different energy bands are presented.

Fe_8N	V_{zz}^{p-p}	V_{zz}^{d-d}	V_{zz}^{val}	Fe_8C	V_{zz}^{p-p}	V_{zz}^{d-d}	V_{zz}^{val}
Fe 3s3p	+2.448	0.000	+2.417	Fe 3s3p	+2.455	0.000	+2.434
N 2s	−4.369	−0.174	−4.554	C 2s	−4.822	−0.354	−5.194
N 2p	−4.552	−2.467	−7.067	C 2p	−2.479	−3.177	−5.695
Fe 3d	+0.686	+7.310	+8.074	Fe 3d	−1.200	+6.309	+5.166
Valence band	−5.787	+4.669	−1.130	Valence band	−6.046	+2.778	−3.289

a large decrease of the d–d contribution. The value of the d–d contribution is almost totally determined by the Fe 3d electrons. In the Fe_8C structure this distribution is more symmetric compared to that in Fe_8N. This more symmetric distribution of Fe 3d electrons in Fe_8C leads to a smaller compensation of the negative contributions from the C 2s and C 2p electrons.

Finally we tried to analyse the reasons for the increase in symmetry of the 3d-band charge distribution in Fe_8C. Let us consider partial contributions to the EFG just for the 3d band. In Fe_8N, the p–p and d–d contributions are both positive and decrease the total (negative) EFG. For Fe_8C the situation is different: the p–p contribution becomes negative and its absolute value becomes twice as large. This decreases the positive d–d contribution and causes the increase of the total EFG.

The results of our calculations also permit us to evaluate such important characteristics of the Mössbauer spectrum as the isomer shift. However, our research led us to the conclusion that this problem needs a separate investigation. At present, a number of experimental results on the isomer shifts in Fe–C and Fe–N fcc alloys exist, but different groups report different values (Foct *et al* 1988, Oda *et al* 1990, 1994, Nadutov 1998, Sozinov *et al* 1999). This fact complicates the comparison and analysis of theoretical and experimental data.

In this paper we present our results for the calculation of the isomer shifts for the Fe_0 and Fe_2 types of atom in the Fe_4N structure. We took the value of the calibration constant $\alpha = -0.27\ a_0^3$ mm s^{-1}, which was calculated by comparing theoretical densities at the nuclei and experimental isomer shifts for six different Fe compounds (Timoshevskii *et al* 2001). The values obtained for the isomer shifts are $\delta_0 = 0.40$ and $\delta_2 = 0.42$ for the Fe_0 and Fe_2 atoms respectively. These values are in good agreement with the experimental isomer shifts, $\delta_0^{expt} = 0.39$ and $\delta_2^{expt} = 0.45$, obtained by Rochegude and Foct (1986). A detailed analysis of experimental and theoretical values of the isomer shifts in Fe–C and Fe–N fcc alloys will be given in our next paper (Timoshevskii *et al* 2001).

5. Summary

The results of our full-potential band-structure calculations of Fe_4N, Fe_8N and Fe_8C structures led to the following conclusions. We obtained theoretical values of the lattice parameter, magnetic moments, quadrupole splitting and isomer shifts for the iron nitride Fe_4N structure. All results are in good agreement with experimental data.

The lattice parameters, magnetic moments and quadrupole splittings were calculated for the Fe_8N and Fe_8C superstructures, which were chosen as models for Fe–N and Fe–C fcc alloys. Analysis of the density of electronic states for both structures permits us to reach the conclusion that in Fe_8C the chemical Fe–C bonding is more covalent than the Fe–N bonding in Fe_8N. Fe–C austenite can be successfully modelled by the ordered Fe_8C superstructure, containing iron atoms in Fe_0 and Fe_1 configurations. The calculated quadrupole splitting is in good agreement with experimental values.

We performed a detailed analysis of the formation of the EFG at Fe nuclei in this structure. We observe that the main EFG contribution arises from carbon 2s and 2p states. The contributions of these two states appear to be almost equal. The contributions of the carbon states are largely cancelled by the asymmetry of the spatial distribution of the Fe 3d electrons.

We come to conclusion that Fe–N austenite cannot be modelled by the Fe_8N structure. The results of our calculations show that the nitrogen distribution in real Fe–N alloy is different from the nitrogen distribution in the Fe_8N structure.

References

Bauer Ph, Uwakweh O N C and Genin J M R 1988 *Hyperfine Interact.* **41** 555
Bauer Ph, Uwakweh O N C and Genin J M R 1990 *Metall. Trans.* A **21** 589
Blaha P and Schwarz K 1983 *Int. J. Quantum Chem.* **23** 1535
Blaha P, Schwarz K and Herzig P 1985 *Phys. Rev. Lett.* **54** 1192

Blaha P, Schwarz K and Luitz J 1999 *WIEN97, a Full Potential Linearized Augmented Plane Wave Package for Calculating Crystal Properties* Technical University of Vienna, Austria (ISBN 3-9501031-0-4)
Cheng Liu, Böttger A, De Keijser Th H and Mittemeijer E J 1990 *Scr. Metall. Mater.* **24** 509
De Cristofaro N and Kaplow R 1977 *Metall. Trans.* A **8** 35
Dufek P, Blaha P and Schwarz K 1995 *Phys. Rev. Lett.* **75** 3545
Foct J, Rochegude P and Hendry A 1988 *Acta Metall.* **36** 501
Frazer B C 1958 *Phys. Rev.* **122** 751
Gavriljuk V G and Nadutov V M 1983 *Fiz. Metall. Metalloved.* **55** 520
Gavriljuk V G, Nadutov V M and Gladun O 1990 *Phys. Met. Metallogr.* **3** 128
Genin J M and Flinn P A 1968 *Trans. Metall. Soc. AIME* **242** 1419
Jacobs H, Rechenbach D and Zachwieja U 1995 *J. Alloys Compounds* **227** 10
Macedo W A A and Keune W 1988 *Phys. Rev. Lett.* **61** 475
Montano P A, Fernando G W, Cooper B R, Moog E R, Naik H M, Bader S A, Lee Y C, Darici Y M, Min H and Marcano J 1987 *Phys. Rev. Lett.* **59** 1041
Nadutov V M 1998 *Mater. Sci. Eng.* A **254** 234
Oda K, Fujimura H and Ino H 1994 *J. Phys.: Condens. Matter* **6** 679
Oda K, Umezu K and Ino H 1990 *J. Phys.: Condens. Matter* **2** 10 147
Perdew J P, Burke S and Ernzerhof M 1996 *Phys. Rev. Lett.* **77** 3865
Prescia D, Stampanoni M, Bona G L, Vaterlaus A, Willis R F and Meier F 1987 *Phys. Rev. Lett.* **58** 2126
Rochegude P and Foct J 1986 *Phys. Status Solidi* a **98** 51
Singh D 1994a *Plane Waves, Pseudopotentials and the LAPW Method* (Dordrecht: Kluwer–Academic)
Singh D 1994b *Phys. Rev.* B **43** 6388
Sozinov A L, Balanyuk A G and Gavriljuk V G 1997 *Acta Mater.* **45** 225
Sozinov A L, Balanyuk A G and Gavriljuk V G 1999 *Acta Mater.* **47** 927
Timoshevskii A N, Timoshevskii V A and Yanchitsky B Z 2001 Isomer shifts and hyperfine fields in Fe–N and Fe–C fcc alloys, in preparation